

# Three-Stage Power System Restoration Methodology Considering Renewable Energies

Cong Shen<sup>1</sup>

*Kassel University, Wilhelmshoer Allee 73, Germany*

*Paul Kaufmann<sup>a</sup>, Christian Hachmann<sup>b</sup>, Martin Braun<sup>b,c</sup>*

*<sup>a</sup>University of Paderborn, Warburger Str.100, Paderborn, Germany*

*<sup>b</sup>Kassel University, Wilhelmshoer Allee 73, Germany*

*<sup>c</sup>Fraunhofer IWES, Koenigstor 59, Kassel, Germany*

---

## Abstract

This is a study of a combined load restoration and generator start-up procedure. The procedure is structured into three stages according to the power system status and the goal of load restoration. Moreover, for each load restoration stage, the proposed algorithm determines a load restoration sequence by considering renewable energy such as solar and wind park to achieve objective functions. The validity and performance of the proposed algorithm is demonstrated through simulations using IEEE-39 network.

*Keywords:* load restoration, restoration stage, renewable energy, voltage/frequency fluctuations

---

## 1. Introduction

With the development of modern societies, power supply reliability becomes one of the most important issues for today's network operators. The blackout state of a power system is defined as the interruption of electricity generation, transmission, distribution and consumption, when operation of the transmission system or a part thereof is terminated. A power system blackout can cause serious consequences by restricted operation of medical facilities, road, air, and

---

<sup>1</sup>Corresponding author: Cong Shen; Email: cong.shen@uni-kassel.de

rail traffic congestion, internet breakdown, and interruption in manufacturing processes, etc. Normally, most of the supply interruptions are caused by temporary failures such as lighting, overhead line swing, etc. which can be removed by protection relays. However, incorrect handling of failures may lead to cascading outage which eventually results in a partial to complete collapse. To reduce the economical impacts and minimize the negative influences brought by power system blackout, an efficient power system restoration plan is of utmost importance for power system recovery.

A power plant can be classified as Non-Black Start (NBS) and Black Start (BS) unit. A NBS unit has to receive cranking power to start its auxiliary devices before rebooting, while BS unit can reboot itself without external power. In the initial power system restoration process without tie line, the primary task is to reboot BS units to send cranking power to start NBS units. Normally, during the booting process, the BS units, such as hydro power plants are utilized to control frequency and voltage due to their fast response speed. In some cases, the output of BS units decreases in order to keep the frequency and voltage stable. Under normal conditions, the booting process of NBS units, whose output increases almost linearly, dominates the power system restoration time as the booting process of NBS units is much longer than the BS units. Depending on status and characteristics of NBS units, start-up sequence of NBS units has to be determined, which influences power system restoration time. After that, the skeleton of network should be energized to make a good foundation for massive load restoration. This study is towards load restoration process whose main task is to determine the sequence and the amount of load that can be picked up in one step. In each load restoration step, the active power of restored load must be limited according to the active output of online generators or else the constraints of frequency stability cannot be satisfied. In similar way, to ensure voltage stability, the online generators have to have enough reactive power reserve to balance the reactive power of restored load. Besides the control systems of online generators, such as the excitation systems, turbine governors, etc, the static and dynamic behavior of load have great impact on the frequency

and voltage deviations during the load restoration process.

## 2. Overview of Three-Stage Load Restoration Process

Power system restoration subdivides into build-up and build-down strategies [1, 2], and consists of tasks such as start-up of generators, energizing unloading transmission lines and load restoration. In [3, 4, 5, 6, 7], general challenges and guidelines for a network restoration process are discussed. According to [3, 4], power system restoration can be divided into three steps: booting generators, energizing the network skeleton, and load restoration. Based on these three steps, the overall load restoration process is classified into three stages in this paper as illustrated in Fig. 1.

1. Normally, BS units are hydro power plants, diesel generators, etc. with limited capacity. At the beginning of power system restoration, NBS units (such as fossil fuel power plant) with large capacity have to be restarted and re-connected to grid. Therefore, the main objective in this stage is to send cranking power to NBS units that can be energized by BS unit. The number of NBS units that can be rebooted simultaneously in this stage is determined by the capacity of BS unit. In this stage, the entire power system suffers from blackout. BS unit has to restart immediately and energize the network between BS and NBS units. Generally, most of BS units require to reach the minimal output as soon as possible to ensure stable operation. Therefore, the primary task of load restoration in this stage is to restore commensurable load, that is not less than the minimal output of BS unit. Since the main task in this stage is to reboot NBS units, the load restoration process halts when the restored load approaches the maximal restorable load (except cranking power of NBS units) in this stage.
2. In this stage, some NBS units are booting or waiting for the cranking power from grid, while the output of online generators increases. During the waiting period of connection of NBS units, the increased output of

online generators can be used to re-energize the important load center substations. The goals of second stage are the followings:

- energizing the network skeleton to next NBS units,
- sending cranking power to NBS units and picking up load for stable operation of power system,
- connecting additional high priority load when the full network skeleton is energized and all NBS units can receive cranking power from grid.

3. After re-energizing all substations and NBS units in the grid, the load restoration enters into the third stage whose main task is to restore as much load as possible within minimal time. In the third load restoration stage, the load restoration process can be conducted by determining the load restoration sequence based on the load priority and load size. The third load restoration stage terminates when all load in the grid is restored or the maximal capacity of generators is reached.

The contributions of this paper are:

- Define three load restoration stages according to status of power system restoration process. In each stage, the tasks and goals of load restoration are defined.
- In each load restoration stage, a load restoration methodology is developed to achieve the goal functions and satisfy the operational constraints.
- A novel algorithm is proposed based on fuzzy system to determine the energizing sequence of the network skeleton.
- Determine the negative/positive spinning reserve power by considering the renewable energy.
- Determine the minimal/maximal restorable load by considering generator start-up sequence.

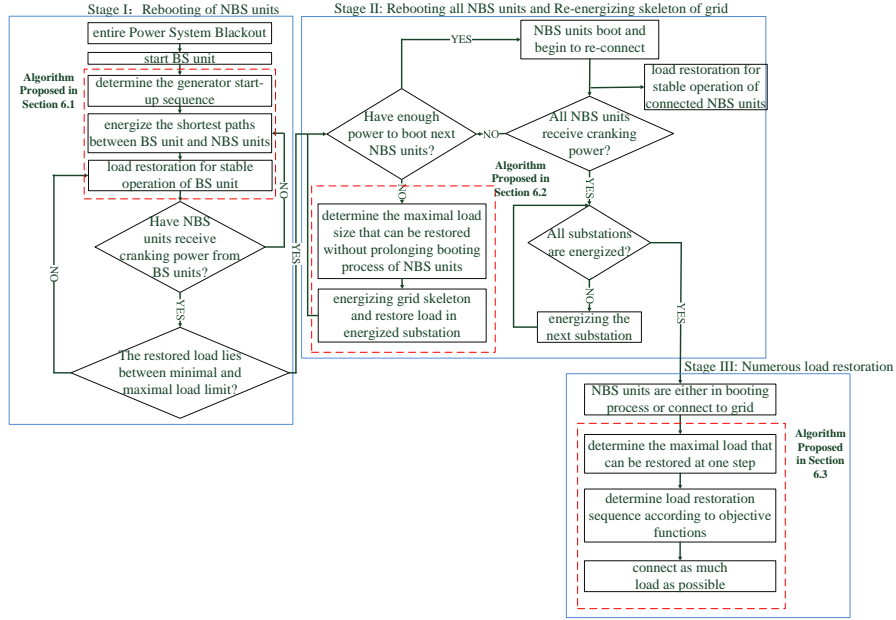


Figure 1: Power System Restoration Stages and Tasks

- Consideration of renewable energy as NBS units
- Integrating dynamic simulations to check on transient stability criteria

The limitations of this paper are:

- This paper focuses on load restoration process for the situation that total power system is blackout and the collapsed grid can not receive external power via tie line.
- A large scale grid has to be partitioned into small subsystems to enable parallel restoration process in each subsystem [8]. Normally, the partitioning strategies have ensured that each subsystem includes only one BS unit. Since the load restoration process in each subsystem is similar, we only focus on the load restoration in one subsystem in this paper.

### 3. Related Work and Paper Contributions

Since the load restoration problem can be formalized as a multi-objective optimization problem, in [9] an ant algorithm is implemented to determine the load restoration sequence by considering cold load phenomena. In [10], distributed generation (DG) is considered to support the power system restoration and optimized by using genetic algorithm. In [11], fuzzy-heuristic methodology is implemented to calculate the restoration time by considering electric service quality (ESQ) index. The goal of this paper is to minimize the economic loss which is related to penalty costs caused by non-supplied energy. The similar work [12] utilizes the fuzzy set theory to estimate the loads in distribution network without real time meters. Based on the estimated value, a heuristic search method is proposed to establish the restoration plan. The goal of the restoration plan is to minimize the switching operations. In [13], the status of each switch in distribution network is represented as a bit in a chromosome for genetic algorithm (GA). Each chromosome maps to feasible network topology. The optimal distribution network topology can be figured out by using GA after faults occur. Paper [14] implements the particle swarm algorithm to find optimal sizing and location of distribution generation (DG) in distribution network to reduce the distribution substation transformer loss and the lost load. In [15], a tabu search based metaheuristic technique is implemented to calculate the restoration time by considering multiple objectives, such as maximization of the transferred load, minimization of the required time and of the power losses of the new configuration. In [16], a load estimation method based on the wide area monitoring system (WAMS) is proposed to determine maximal load size that can be restored in one step. The range of restorable load size is updated iteratively by the frequency error between the calculated frequency and the measured frequency from WAMS. Nevertheless, the mentioned contributions only consider the situation how to pick up the load optimally when part of restored network is stable. Moreover, the contributions and operation constraints of renewable energy in the load restoration process are not considered

during the load restoration process. The innovation and contribution in this paper is the consideration of renewable energy in load restoration and to keep power system stability in terms of voltage and frequency transients during the restoration process starting with the first blackstart unit. Tab. 1 compares the proposed algorithm and the existing researches by using six main features.

This paper is organized as follows: Section 4 provides the mathematical model of the power system for conducting dynamic simulations. In section 5, the operation constraints for load restoration are given. Section 6 explains the task oriented algorithms for three load restoration stages. Section 7 presents the simulation results for the IEEE 39 nodes test grid. Finally, Section 8 concludes the paper.

#### 4. Mathematical model of power system

In order to calculate the transient behavior of frequency and voltage fluctuations after restoring a load, the complete mathematical model of the overall system has to be established. This mathematical model consists of the differential equations and algebra equations. Differential equations describe the dynamic models of online generators and restored load while algebra equations describe the network equations of network topology, static load, and generator equations. The mathematical models which are utilized in this paper for transient simulation are depicted as follows:

**Synchronous Generator Model:** The second-order synchronous generator model is used for transient simulation, as it is sufficient for the estimation of frequency and voltage deviations [25]. According to the recommendation in [26], IEEE standard 421.5 is implemented for excitation system model. The configurations and parameters of excitation system model are presented in [25]. Moreover, the turbine and turbine governor model which are described in [25] are implemented according to the conclusion in [27].

**Load Model:** The load composition varies with time and has large randomic-

Table 1: Comparison results of proposed algorithm and existing researches

Reference	F1	F2	F3	F4	F5	F6
This work	Y	Y	Y	Y	Y	Y
[17]	N	N	N	N	Y	N
[18]	N	Y	N	N	Y	N
[19]	N	Y	N	N	Y	N
[20]	N	N	Y	N	N	N
[21]	N	N	N	N	Y	N
[22]	N	N	N	N	Y	N
[23]	N	Y	N	N	Y	N
[24]	N	Y	N	N	Y	N

**Feature:**

F1: Does the method consider renewable energies during the load restoration?

F2: Does the method provide the load restoration sequence?

F3: Does the method calculate the maximal restored load in different power system status?

F4: Does the method handle the total power system blackout?

F5: Can the method be employed without training?

F6: Does the method restore load with different task according to power system status?

**Notation:**

Y: Yes.

N: No.



ity. In this paper, the composite load model which combines ZIP (Eq. 1) and induction motor model is implemented. The ZIP and induction motor represent the static and dynamic part of load respectively. Load model parameters can be estimated by the historic data using load forecasting algorithm. Moreover, the cold load model in [10] is implemented to simulate the cold load phenomenon.

$$\begin{aligned} P_r &= P_{or} * [K_{PZ} * (U_r/U_{or})^2 + K_{PI} * (U_r/U_{or}) + K_{PP}] \\ Q_r &= Q_{or} * [K_{QZ} * (U_r/U_{or})^2 + K_{QI} * (U_r/U_{or}) + K_{QP}] \end{aligned} \quad (1)$$

where  $P_r$ ,  $Q_r$  and  $U_r$  are real active, reactive power and voltage values of load;  $P_{or}$ ,  $Q_{or}$  and  $U_{or}$  are the rated values of active, reactive power and voltage of load;  $K_{PZ}$ ,  $K_{PI}$  and  $K_{PP}$  are the active power parameters of load mode with  $K_{PZ} + K_{PI} + K_{PP} = 1$ ;  $K_{QZ}$ ,  $K_{QI}$  and  $K_{QP}$  are the reactive power parameters of load mode with  $K_{QZ} + K_{QI} + K_{QP} = 1$ .

**Inverter Model:** A PQ control strategy is implemented for the inverter model. Under PQ control strategy, the output of active and reactive power from distribution generators (DG) are controllable.

## 5. Operational Constraints for Load Restoration

To ensure stable operation of the power system, the following constraints have to be satisfied during the overall load restoration process:

- The steady state voltage fluctuation has to lie in the prescribed ranges

$$V_{min} \leq V_i \leq V_{max}, \quad i = 1, \dots, N_s, \quad (2)$$

where  $V_{min}$  and  $V_{max}$  are the minimal and maximal allowable steady state voltage,  $V_i$  is the steady state voltage at  $i_{th}$  substation,  $N_s$  is the number of substations.

- The maximal transient voltage fluctuation should lie in the acceptable range

$$V_{tmin} \leq V_{ti} \leq V_{tmax}, \quad i = 1, \dots, N_s, \quad (3)$$

where  $V_{t_{min}}$  and  $V_{t_{max}}$  are the minimal and maximal allowable transient voltage,  $V_{ti}$  is the transient voltage at  $i_{th}$  substation.

- The current within the restoration paths should not exceed the maximal value

$$I_j \leq I_{max}^j, \quad j = 1, \dots, N_e, \quad (4)$$

where  $N_e$  is the number of lines and transformers in restoration paths,  $I_{max}^j$  is the maximal allowable current in  $j_{th}$  line and  $I_j$  is the current in  $j_{th}$  line.

- In power system, frequency control consists of three stages: primary, secondary and tertiary frequency control. For the primary control, it exists the steady state frequency error due to the proportional control characteristic. In order to bring the frequency back to the normal value, the secondary frequency control is carried out. In interconnected power system, automatic generation control (AGC) is implemented to adjust the reference value of the generators output.

$$|\Delta f| \leq \sigma_t \quad (5)$$

where  $|\Delta f|$  is the maximal frequency fluctuation,  $\sigma_t$  is the allowable transient frequency fluctuation.

- The load has to be restored step-by-step by closing the switches. Thereby, the restored load is not a continual value but a set of discrete values. The maximal load that can be restored at one step should not be exceeded. The constraints of maximal frequency and voltage deviations determine the maximal load that can be restored at one step. Fig. 2 shows the frequency behavior after load restoration. However, to determine the maximal load increment is a complicated task. It depends on the load types, the network topology, excitation and the speed governor systems of the online generators, etc. In [3], it figures out that if the maximal load increment does not exceed 5% rated capacity of online generators, power system can keep

frequency and voltage stable. Moreover, in each load restoration stage, the maximal load increment is limited by the maximal ramp rate of online generators (including NBS and BS). For example, PJM Interconnection (PJM) uses 5% for fossil steam units, 15% for hydro units, and 25% for combustion turbines [28]. In this paper, the maximal load increment is determined by the ramp rate of online generators.

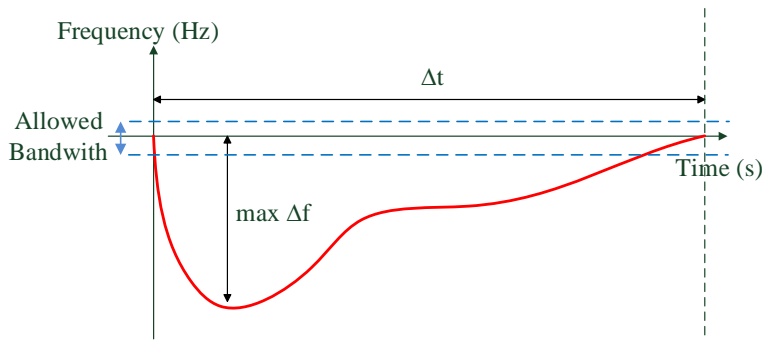


Figure 2: Frequency behaviour after load restoration

- At present, conventional generations, such as thermal power plants, hydro power plants are worked as NBS and BS units. However, based on the forecasting technology, RES can be regarded as BS unit based on the energy availability. For example, for 100 MW solar park, the forecasting minimal output for next 1 hours is 80 MW. Then we can consider this solar park as 50 MW BS unit for next 1 hours. (we should estimate the restoration time to identify the forecasting time schedule of renewable energy, or else this BS unit is only available for 1 hour). Furthermore, the RES equipped with storage can be regarded as BS unit depends on the SOC of storage and the availability of renewable energies. Determination of reserve power for frequency control has to consider many aspects such as maximal fluctuation of restored load and forecasting error of renewable energy output. For example, when a solar park begins to inject power to

grid, commensurable load has to be restored to keep frequency and voltage stable. However, the difference between estimated and actual output of solar park has to be covered by conventional power plants. For the case that the actual output of renewable energy is larger than the forecasting value. This means that other generators in power system have to decrease their output to balance the load and generation. On the other hand, the power system has to have enough positive reserve power to control frequency when the forecasted output is larger than actual output of the solar park. The reserve power has to satisfy Eq. 6 for a forecasting time span  $T_{forecasting}$ .

$$\begin{aligned}
 P^N &\geq \sum_{i=1}^{N^e} P_{n_i} + \sum_{k=1}^{N^l} P_{l_k} \\
 P^P &\geq \sum_{i=1}^{N^e} P_{p_i} + \sum_{k=1}^{N^l} P_{c_k}
 \end{aligned} \tag{6}$$

where  $P^N$  is the negative active power reserve provided by conventional BS/NBS units with primary and secondary frequency control,  $P^P$  is the positive active power reserve provided by conventional BS/NBS units with primary and secondary frequency control,  $P_{n_i}$  is maximal negative fluctuation of  $i_{th}$  renewable energy,  $P_{l_k}$  is maximal negative fluctuation of  $k_{th}$  load,  $P_{p_i}$  is maximal positive fluctuation of  $i_{th}$  renewable energy plant,  $P_{c_k}$  is maximal positive fluctuation of  $k_{th}$  load,  $N^e$  is the number of renewable energy plants,  $N^l$  is number of loads. In addition, power system should have enough reactive power reserve by using reactive compensation devices or the generators which can control their reactive power. The active and reactive power reserve have to be updated for each forecasting time span  $T_{forecasting}$ .

- The ramp rate of online generators has to be larger than the summation of positive/negative reserve power and load increment in one step.

$$G_{rp} \geq \max(P^P, P^N) + L_{in} \tag{7}$$

where  $G_{rp}$  as the ramp rate of online generators,  $L_{in}$  as the load increment in one step.

- The maximal restorable load  $L^{ru}$  has to satisfy Eq. 8, which ensures that enough cranking power is available to reboot all NBS units.

$$L^{ru} \leq \sum_{i=1}^N B_{g_i} + \sum_{j=1}^M N_{B_{b_j}} - P^P - \sum_{k=1}^Q N_{B_{c_k}} - L_{rd} \quad (8)$$

where  $B_{g_i}$  as the maximal active output of  $i_{th}$  BS unit,  $N$  as the number of BS units,  $N_{B_{b_j}}$  as the maximal active output of  $j_{th}$  NBS unit,  $M$  as number of NBS unit that have already integrated into grid,  $N_{B_{c_k}}$  as the cranking power of  $k_{th}$  NBS unit that is still waiting for the cranking power,  $Q$  as the number of NBS units that are under booting process,  $L_{rd}$  as already total restored load.

The minimal restorable load increment  $L_{rl}$  has to satisfy Eq. 9.

$$\sum_{c=1}^W G_{min_c} + P^N = L_{rl} \quad (9)$$

where  $G_{min_c}$  as the minimal active output of  $c_{th}$  online generator,  $W$  as the number of online generators.

**For example**, assuming there are six generators. Generator 1 is a 15 MW BS unit and Generators 2 to 6 are NBS units. Moreover, the generator start-up sequence is from 2 to 6. Tab. 2 shows the generator data of NBS units.

From Tab. 2 can be seen that BS unit can reboot NBS units 2 and 3 simultaneously. After Generator 2 and 3 receive cranking power, the maximal restorable load can not be larger than 153 MW which is calculated by

Table 2: Generator Data of NBS units

Generator	Maximal Output(MW)	Cranking Power(MW)	Minimal Output (MW)
1	15	0	0
2	220	7	40
3	125	4	25
4	220	7	35
5	330	10	60
6	330	10	60

following equation:

$$L^{ru} \leq B_g + N_{B_{b_2}} + N_{B_{b_3}} - P^P - N_{B_{c_4}} - N_{B_{c_5}} - N_{B_{c_6}}$$

with

$$\begin{aligned} B_g &= 15MW, N_{B_{b_2}} = 220MW, N_{B_{b_3}} = 125MW \\ N_{B_{c_4}} &= 7MW, N_{B_{c_5}} = 10MW, N_{B_{c_6}} = 10MW \\ P^P &= 180MW \end{aligned}$$

The minimal restorable load equals 115 MW when Generator 2 and 3 are integrated into grid.

$$G_{min_2} + G_{min_3} + P^N = L_{rl}$$

with

$$G_{min_2} = 40MW, G_{min_3} = 25MW, P^N = 50MW$$

## 6. Three-Stage Load Restoration Methodology

### 6.1. Stage I: Selection of Restoration Paths and Rebooting of NBS units

The main objective in Stage I is to reboot as many NBS units as possible with respect to the capacity of the BS unit. In this stage, BS unit begins to reboot

and send cranking power to NBS units via shortest restoration paths. Before this, the start-up sequence of NBS units has to be determined [29]. The output of BS units should not fall below the minimal output to maintain the stable operation. In order to keep the frequency and voltage deviations within the acceptable range, sufficient load (except cranking power of NBS units) within the restoration path has to be restored. The flow chart of Stage I is illustrated in Fig. 1. In this section, the detailed load restoration algorithm in Stage I is presented. With  $N^s$  as the number of substations in the restoration paths,  $L_{rd_i}$ ,  $\frac{PH_i}{L_i}$  as the total restored load and ratio of load with high priority in the total restored load in  $i_{th}$  substation,  $i = 1, \dots, N^s$ , the objective functions of load restoration in the first stage can be formulated as:

$$\begin{aligned}
 F_1 &= \max \sum_{i=1}^{N^s} (L_{rd_i}) \\
 F_2 &= \max \left( \sum_{i=1}^{N^s} \left( \frac{PH_i}{L_i} \right) \right).
 \end{aligned} \tag{10}$$

The total restored load  $F_1$  should not exceed the  $L^{ru}$  which is calculated by Eq. 8. The detailed calculation steps are explained as follows:

1. The start-up sequence is determined by using the methodology in [29].
2. The number of NBS units is identified according to the capacity of BS unit. This stage is accomplished when all NBS units which can be rebooted by BS units have received cranking power.
3. The shortest restoration paths between BS unit and the goal NBS units are calculated by using Dijkstra's algorithm [30]. The load within the restoration paths  $L_{rp}$  is identified.
4. The lower limit of the restorable load size  $L_{rl}$  equals Eq. 9, while the maximal load size that can be picked up in this phase is calculated by Eq. 8.
5. The maximal load  $PI_{max}$  that can be restored at one step is estimated as 5% rated capacity of online generators.

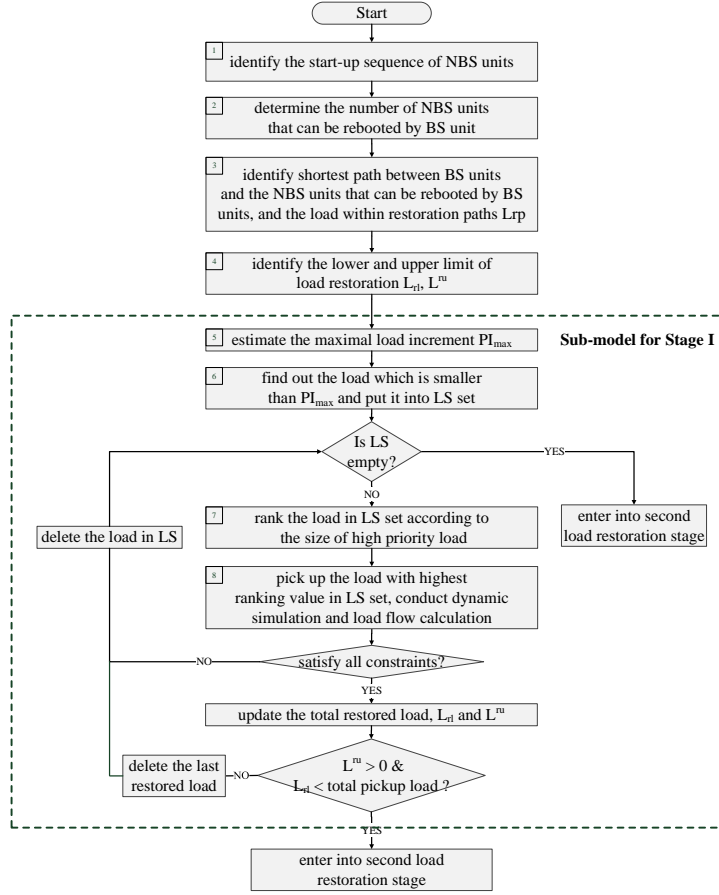


Figure 3: Load Restoration Algorithm in First Stage

6. Only the load in  $L_{rp}$  that is smaller than  $PI_{max}$  is selected and saved in the LS set.
7. If the LS sets is not empty, the load in LS sets is ranked according to load priority. The higher the load priority is, the higher ranking value the load has. Otherwise, the load restoration enters into second stage.
8. The load with highest ranking value will be restored. The transient simulation and load flow calculation are executed to calculate the steady state/transient frequency and voltage fluctuations after picking up this load. Based on the simulation results, if the frequency or voltage fluctua-



tions exceed the tolerance range, this load is deleted from the LS set and total restored load remains unchanged. Or else the total restored load should add this load. If the total restored load is smaller than  $L_{rL}$ , the algorithm continues searching the next load in the LS set. However, if the updated total restored load is larger than  $L^{ru}$ , the load which is restored in the last step has to be shed and deleted in the LS set.

### 6.2. Stage II: Re-energizing the full skeleton of grid

After finishing the first load restoration stage, the restoration paths between BS unit and the NBS units are energized and the initial restored network is created. Based on this restored network, the increased output of online generators can be used to re-energize the skeleton network which consists of most important load center substations and lines. Re-energizing of the important substations in this stage makes good foundation for the massive load restoration in the third stage. In order to determine the optimal network re-energizing sequence, Fuzzy Decision Method (FDM)-Analytic Hierarchy Proces (AHP) algorithm [29] is implemented to calculate the ranking values of candidate substations by considering the node importance degree, the load priority in substation, and shortest path between restored network and substations. Meanwhile, the load in the energized substations is selected to be restored by considering the load priority and available power of online generators.

#### 6.2.1. Performance Indexes for Establishing Network Skeleton

In order to determine the ranking values of candidate substations, three performance indexes are introduced as follows:

**Node Importance Degree  $\alpha_i$ :** The overall network can be regarded as a graph in which the nodes represent substations and the graph connections stand for lines. The node importance degree  $\alpha_i$  of node  $i$  is defined according to [31] as

$$\alpha_i = \frac{1}{n_i e_i}, \quad (11)$$

$$e_i = \frac{\sum_{i,j \in v_i} d_{min,ij}}{n_i(n_i - 1)/2}. \quad (12)$$

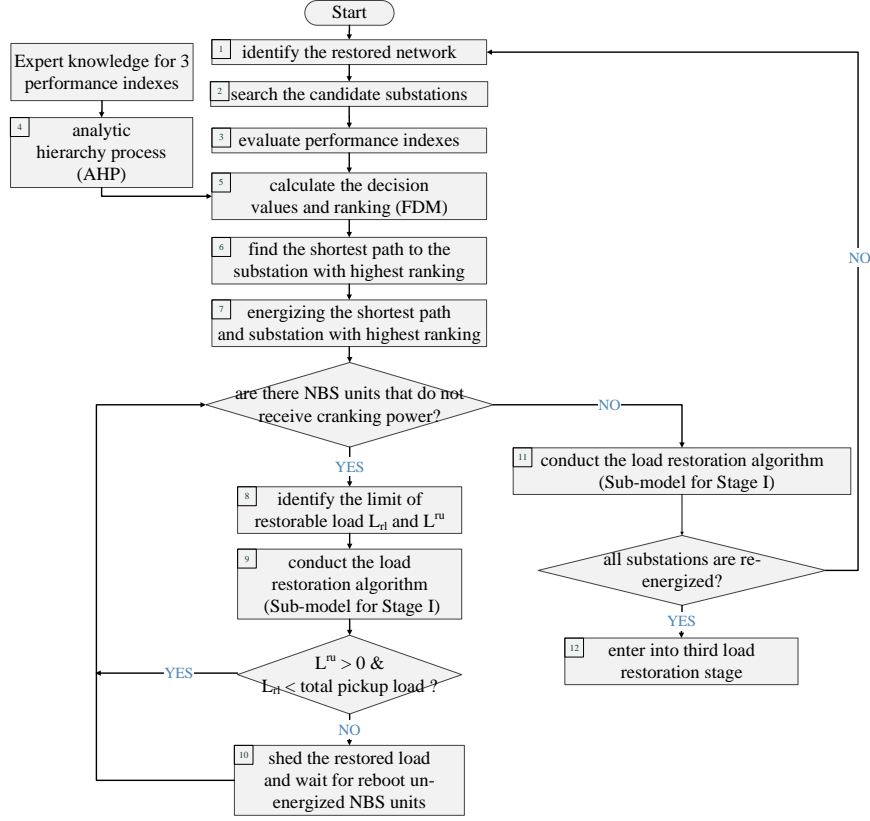


Figure 4: Load Restoration Algorithm in Second Stage

In original network, the nodes which connect to node  $i$  are combined with node  $i$ . After the contraction,  $n_i$  in Eq. 11 is the total number of nodes in the new network,  $e_i$  is the average of the shortest distances,  $v_i$  is the total number of nodes in the original network, and  $d_{min,i,j}$  is the shortest distance between node  $i$  and node  $j$ . The smaller the node number after  $i_{th}$  node contraction, the more important  $i_{th}$  node is. On the other hand, the value  $e_i$  evaluates the network change degree after  $i_{th}$  node contraction. The smaller the  $e_i$ , the more important  $i_{th}$  node is.

**High Priority Load Size  $\frac{PH_i}{L_i}$ :** The ratio of the load with high priority to the total load in the  $i_{th}$  substation  $\frac{PH_i}{L_i}$  is also an aspect that can assess the importance degree of the substations. The value of  $PH_i$  and  $L_i$  can be

estimated by the historic load curves.

**Length  $L_i$ :** The shortest line length  $L_i$  between the restored network and the  $i_{th}$  candidate substation influences the reactive power and voltage regulation during the load restoration process. The shorter the line length, the better the substation.

### 6.2.2. Load Restoration Algorithm in Stage II

The detailed calculation steps of proposed load restoration algorithm are shown in Fig. 4:

1. At the beginning of the algorithm, the restored network topology is identified.
2. In the second step, all un-energized substations are regarded as candidate substations. In succeeding restoration path update, substations that are selected to be re-energized by restored network are added successively to the network skeleton. In each update step, only one substation is added. After the update, the selection rankings for the remaining candidate substations are recomputed in step 3 to 5 in Fig. 4.
3. To be able to select one substation among the candidate substations, the performance indexes have to be evaluated for all the candidate substations.
4. The priorities are given as ranking for all performance index pairs. To harmonize the priority ranking and solve priority conflicts, the analytic hierarchy process (AHP) [32] is used to calculate weighting factors of performance indexes.
5. Given the performance indexes and their priorities, in step 5 a multi-objective fuzzy decision method (FDM) is executed to establish a non-dominated set and a linear ordering on it [33]. For FDM, the performance indexes have to be formalized as fuzzy membership functions. Since the values of performance indexes  $\alpha_i$  and  $\frac{PH_i}{L_i}$  are lying between 0 and 1, and the higher the better, linear monotonic increased membership functions can be used. For the distribution line lengths, linear monotonic decreased

membership functions can be employed. The line lengths have to be normalized before. FDM computes a set of non-dominated solutions and ranks the solution using the decision values.

6. The shortest path between the restored network and the candidate substation with the highest ranking value can be identified by using Dijkstra algorithm.
7. The restored network topology is updated by energizing the selected candidate substation and restoration paths.
8. The limit of restorable load  $L_{rl}$  and  $L^{ru}$  should be updated by Eq. 8 and Eq. 9 if the number of online generators changes.
9. The load restoration is conducted by using the load restoration algorithm in the first load restoration stage (Sub-model for Stage I).
10. If the restored load exceeds the upper limit of restorable load  $L^{ru}$ , the load restoration procedure has to suspend until new NBS units begin to inject power to grid. Meanwhile, the loop ends when all NBS units have received cranking power.
11. If all the NBS units have received the cranking power, the load restoration process continues by using the Sub-model for Stage I.
12. The second load restoration process terminated when all the NBS units receive the cranking power and all substations are energized.

### 6.3. Stage III: Numerous load restoration

After all NBS units have received cranking power and all substations and lines are energized, the goal of load restoration is to pick up as much load as possible within the minimal time. This problem can be formulated as knapsack problem [34]. Many optimization algorithms including dynamic programming [35], greedy algorithm [34], evolutionary algorithm [36] are used to solve this problem. In this restoration stage, the restorable load which is limited by maximal load increment is ranked according to the high priority load size. Before picking up load, the transient simulation and load flow calculation are executed to check the operation constraints. After that, greedy algorithm is

implemented to determine the load restoration sequence. Fig. 5 indicates the flow chart of the load restoration process in third stage.

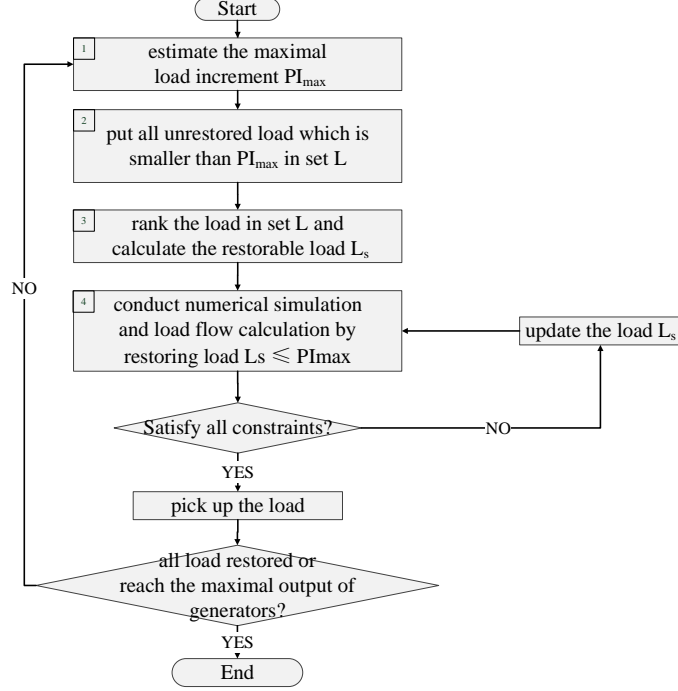


Figure 5: Flow Chart of Third Load Restoration Algorithm

The detailed calculation process is explained as follows:

1. The maximal load increment  $PI_{max}$  is determined.
2. The unrestored load which is smaller than  $PI_{max}$  is put into the set L.
3. The load in set L is ranked according to the load priority and load size. The load with high priority and large size has high ranking value. The load set  $L_s$  that can be restored in one step is calculated by Eq. 13.

$$L_s = \max \sum_{i=1}^N L_i^d, N \leq M \quad (13)$$

with

$$L_s \leq PI_{max}$$

where  $L_i^d$  is the  $i_{th}$  load size in L set, M is the total number of unrestored load in L set and i is the ranking value index.

4. Transient simulation and load flow calculation are executed to calculate the frequency and voltage deviations and check the steady state operation constraints after restoring  $L_s$ .
5. If all operation constraints lie in the acceptable range after load restoration, the load can be picked up.
6. If same constraints can not be satisfied, the load with lowest ranking value in  $L_s$  should be deleted and the transient simulation and load flow calculation have to be conducted again with updated  $L_s$ . The load restoration process terminates when all load is restored or the maximal output of generators is reached.

## 7. Experiments and Results

In this section, the new England network with 39 nodes illustrated in Fig. 6 is used to demonstrate the proposed load restoration algorithm. The software Digsilent PowerFactory 14.0 is used to execute the power system dynamic simulations and calculate the frequency and voltage fluctuations after load restoring.

In order to demonstrate the load restoration process more clearly, we make following modifications and assumptions for the new England 39 nodes network:

- Generator 1 is a hydraulic power plant with 150 MW rated capacity and regarded as a BS unit. The hydraulic turbine governor and excitation systems are selected from the Powerfactory library named "pcuHYGOV" and "vcoIEEET1" respectively. The ramp rate and the minimal output of the Generator 1 is 20 MW/min and 10% of the rated capacity.
- Generator 2 and 9 are thermal power plants with 330 MW, 220 MW rated capacity and regarded as NBS units. The steam turbine governor and excitation systems are selected from the Powerfactory library named "GOV" and "AVR" respectively. Generator 3 is a wind park with 50 MW rated capacity. The generator data is shown in Tab. 3.

Table 3: Data of Generator 2, 3 and 9

Generator	Maximal Output(MW)	Minimal Output(MW)	Rebooting Time (min)	Cranking Power(MW)	Ramp Rate (MW/min)
2	330	85	80	10	16.5
9	220	70	100	7	11
3	50	0	10	2	5

- Generator 4 to 8, and 10 are eliminated and replaced by the load.
- To simplify the simulation, the maximal load fluctuation is assumed as  $\pm 10\%$  of restored load.
- According to the algorithm in [29], the optimized generator start-up sequence is generator 2,9 and 3.
- The new England grid is regarded as 110 kV network
- The fluctation of wind park is assumed as  $\pm 5\%$ .
- The necessary operation time for energizing a line is assumed to be 5 minutes.
- The forecasting time span for wind park is assumed to be 5 minutes.
- The necessary time for load restoration step is assumed to be 5 minutes.
- The load model parameters are generated randomly within the acceptable ranges.

### 7.1. First Load Restoration Stage

In the first restoration stage, the Generator 1 begins to restart and energize the restoration paths 39-9-8-7-6-31 in order to send the cranking power to Generator 2. The red line in Fig. 6 shows the restoration paths. The load compositions and size within the restoration paths are illustrated in the Tab. 4. The lower limit of the load restoration size equals 16.5 MW according to Eq. 9

( $G_{min1}$  (15 MW) +  $P^N$  (restored load \* 0.1)), while the maximal load that can be restored in this stage can be calculated according to Eq. 8 ( $B_{g1}$  (150 MW) -  $N_{B_{c2}}$  (10 MW) -  $N_{B_{c9}}$  (7 MW) -  $N_{B_{c3}}$  (2 MW) -  $P^P$  (restored load \* 0.1)) -  $L_{rd}$ . Meanwhile, the maximal load increment in one step can be estimated as 20 MW. Tab. 4 indicates that load L1, L3, L4 and L10 can be restored as the size of load is smaller than 20 MW. Tab. 5 shows the load restoration procedure in the first stage. Fig. 7 illustrates output of Generator 1, the frequency and voltage fluctuations respectively.

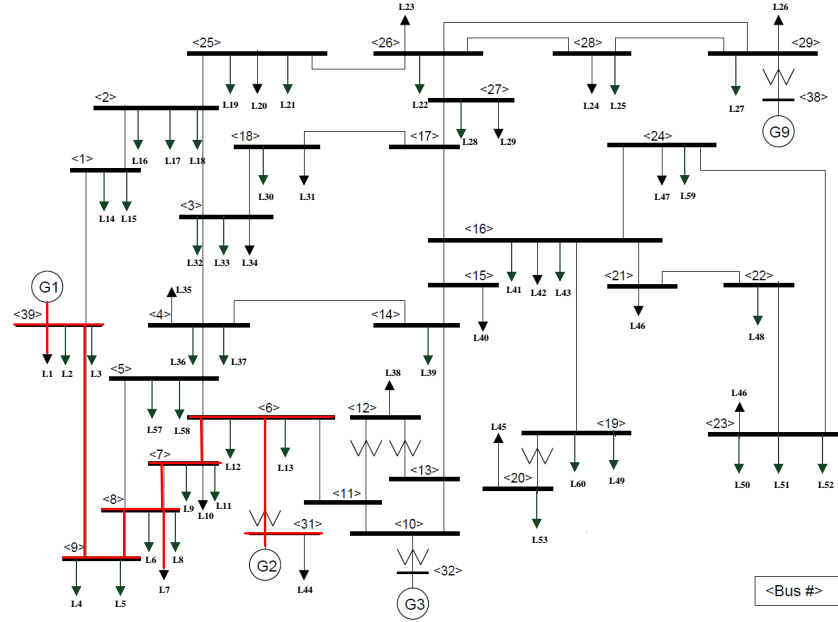


Figure 6: Restoration Paths in First Restoration Stage

## 7.2. Second Load Restoration Stage

At the beginning of second restoration stage, Generator 2 receives the cranking power from Generator 1 and begins to reboot. The next step is to reenergize the shortest restoration path between Generator 1 and Generator 9



Table 4: Load Compositions, Size, and Priority in each Substation

Substation	Load	Total Load(MW)	Static Load(%)	Dynamic Load (%)	Priority
39	L1	19.9	80	20	1
	L2	23.8	90	10	2
	L3	19.7	50	50	2
9	L4	18.4	60	40	1
	L5	22.2	30	70	2
8	L6	24	20	80	2
	L7	20.9	10	90	1
	L8	20	40	60	2
7	L9	37.9	70	30	1
	L10	18	40	60	2
	L11	22.3	20	80	2
6	L12	23	20	80	1
	L13	21.9	90	10	2
31	L44	26.3	20	80	2

Table 5: Load Restoration Procedure in First Stage

Time (Min)	Energized Substations	Restored Load	Total Restored Load (MW)	Goal Substation	$L^{ru}$ (MW)	$L_{rl}$ (MW)
0-5	39	L1	19.9	31	109.11	16.99
5-10	9	L4	38.3	31	88.87	18.83
10-15	8	L3	58	31	67.2	20.8
15-20	7	L10	76	31	47.4	22.6
20-25	6	None	76	31	47.4	22.6
25-30	31	None	76	29	47.4	22.6
Generator 2 receives cranking power from grid						

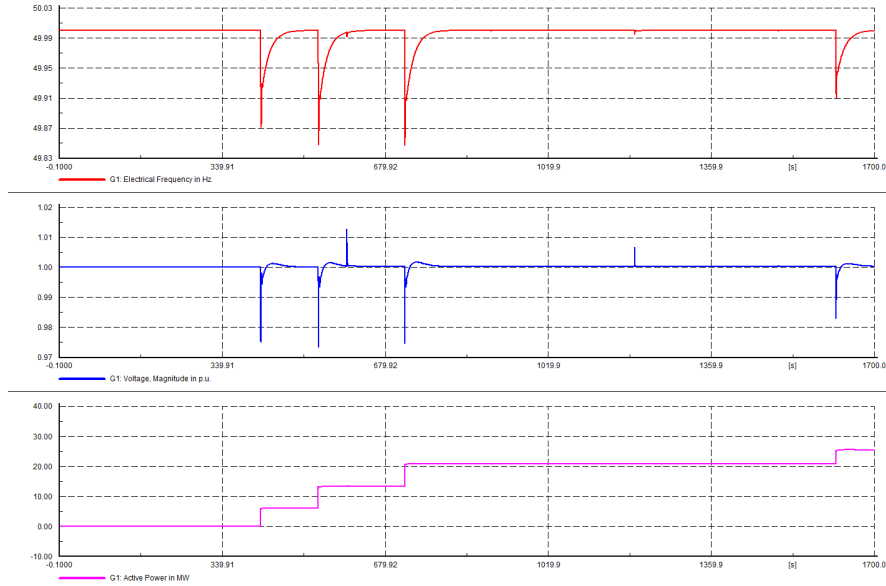


Figure 7: Output of Generator 1, frequency and voltage fluctuations in this first load restoration stage

(39-1-2-25-26-29) to send cranking power to reboot Generator 9. According to the assumption, energizing this restoration path needs 25 minutes. Within this time, the increased output of Generator 1 can be used to pick up the load in the energized substations. After Generator 9 has received cranking power, Substation 10 becomes the goal substation in which Generator 3 has connected. After 75 minutes, Generator 3 begins to inject power into grid. The lower and upper limit of the load restoration size have updated as the  $P^P$  and  $P^N$  have changed in real time (every five minutes in this case) to accommodate the fluctuation output of wind park. Moreover, the minimal available output of wind park during the entire power system restoration process is above 20 MW which can be regarded as stable source.

After 50 minutes, Generator 9 receives the cranking power from grid and begins to reboot. During the booting procedure of Generator 2 and 9, the increased output of Generator 1 can be used to energize the skeleton network

and restore the load with highest priority. After 115 minutes, the Generator 2 begins to inject power into grid and the maximal load increment increases to 41.5 MW. Tab. 6 illustrates the load restoration procedure in this process.

### 7.3. Third Load Restoration Stage

In the third load restoration stage, all the substations are energized. The goal of third load restoration stage is to restore the load as much as possible within the shortest time. The unrestored load is ranked according to the load priority and load size. Tab. 7 illustrates the load restoration sequence in third stage. After 155 minutes, the Generator 9 begins to inject power into grid and the maximal load increment in one step increases to 35 MW. The overall load restoration process ends after 195 minutes.

### 7.4. Simulation Time

Since the voltage and frequency constraints are verified by time-domain simulations by using Digsilent PowerFactory 14.0, the simulation time of proposed algorithm depends on the size of network. Fig. 8 shows the simulation time (one load pickup event) for the IEEE standard network with 9, 14, 39 nodes. The simulation time has the almost quadratic relationship with size of network. However, the large scale network will be partitioned into several subsystems to conduct the network restoration operation. In order to get acceptable simulation time, the size of subsystem should be limited.

### 7.5. Results Comparison

In [37], firefly optimization algorithm (FA) is implemented to calculate the optimal load restoration sequence by considering the renewable energy sources (RES). The difference points between [37] and the proposed three-stage load restoration algorithm are listed in Tab. 8.

Fig. 9 shows the comparison results between proposed three-stage load restoration algorithm and load restoration algorithm in [37]. The proposed algorithm calculates the  $L^{ru}$  and  $L_{rl}$  according to the power system status and forecasting

Table 6: Load Restoration Procedure in Second Stage

Time (Min)	Energized Substations	Restored Load	Total Restored Load (MW)	Goal Substation	Forecasted Wind (MW)	$L^{ru}$ (MW)	$L_{rl}$ (MW)
30-35	1	None	76	29	None	47.4	22.6
35-40	2	L17	85.6	29	None	36.84	23.56
40-45	25	L19,L20	96.2	29	None	25.18	24.62
45-50	26	None	96.2	29	None	25.18	24.62
50-55	29	None	96.2	10	None	25.18	24.62
Generator 9 receives cranking power from grid							
55-60	11	None	96.2	10	None	25.18	24.62
60-65	10	None	96.2	16	None	25.18	24.62
Generator 3 receives cranking power from grid							
65-70	27	L28	114.2	16	None	5.38	26.4
70-75	17	None	114.2	16	None	5.38	26.4
Generator 3 begins to inject power into grid							
75-80	16	L42	130.7	4	20	8.23	28.07
80-85	5	L58	138.93	4	20	0.27	28.89
85-90	4	None	138.1	12	22	0	28.81
90-95	12	None	137.9	23	26	0	28.79
95-100	21	None	138.05	23	23	0	28.8
100-105	22	None	138.93	23	20	0.27	28.89
105-110	23	None	138	18	24	0	28.8
110-115	3	None	137.8	18	28	0	28.7
Generator 2 begins to inject power into grid							
115-120	18	L6,L8 L31,L57	169.8	19	33	304.57	116.98
120-125	19	L49,L33 L18,L7	201.8	24	43	269.82	120.18
125-130	24	L14,L15	235.8	28	39	231.67	123.5
130-135	28	L34, L47	270.8	14	43	192.97	127.08
135-140	14	L43,L60	306.6	15	47	153.45	130.6
140-145	15	L16,L12	<sup>28</sup> 342.6	20	50	113.64	132.2
145-150	20	L52,L48	378.4	13	46	74.46	137.84
150-155	13	L53,L32	414.1	None	48	35.1	141.1
Generator 9 begins to inject power into grid							

Table 7: Load Restoration Procedure in Third Stage

Time (Min)	Restored Load	Total Restored Load (MW)
155-160	L45,L46,L59,L37	452.1
160-165	L2,L9,L44,L51	493.1
165-170	L21, L22,L29,L30	532.7
170-175	L25,L26,L36,L38	571.3
175-180	L5,L39,L40,L41	611.1
180-185	L11, L23,L24,L50	650.8
185-190	L13,L27,L35	688.1

Table 8: Difference Points between algorithm in [37] and Proposed Three-Stage Algorithm

	Algorithm in [37]	Three-Stage Algorithm
RES in Restoration Process	RES begin to start when the whole power system is completely reconstructed.	RES contribute to power system restoration at the beginning of the power system restoration procedure by calculating $P^N$ and $P^P$ .
Restoration Path Selection	The shortest path is selected.	Not only shortest path but also the node importance degree,high priority load size are considered by using FDM-AHP algorithm.

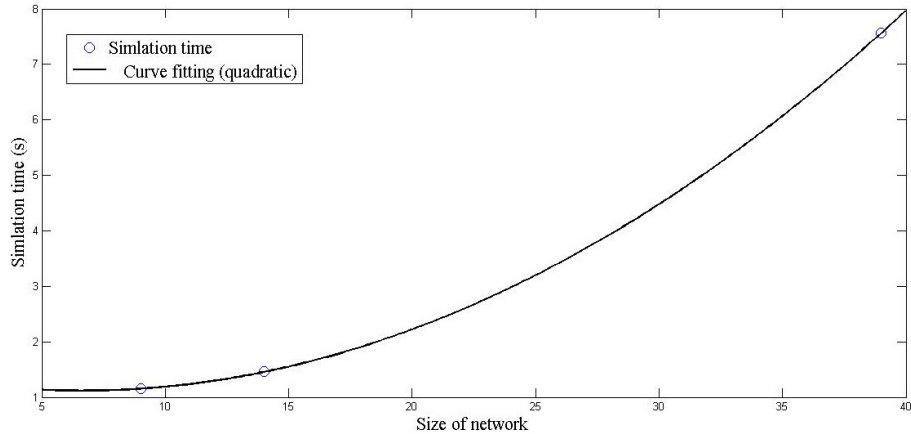


Figure 8: The relationship between restoration time and size of network

wind power. In this way, RES can contribute to the load restoration earlier than the algorithm in [37].

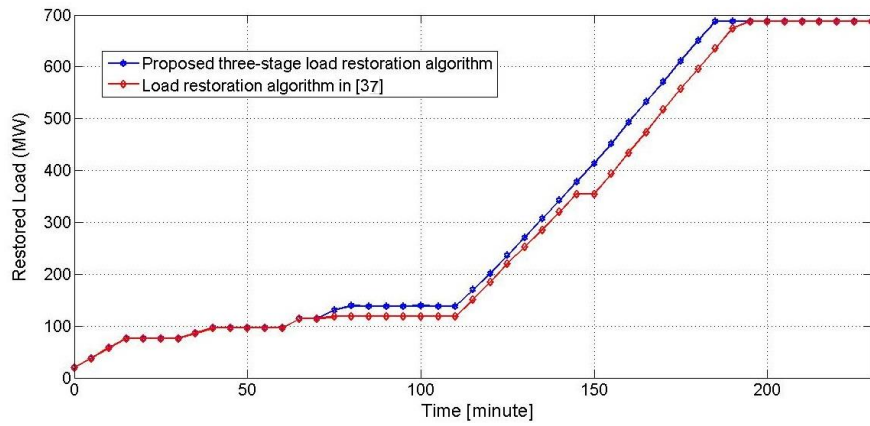


Figure 9: Comparison Results between Proposed Three-Stage Load Restoration Algorithm and Load Restoration Algorithm in [37]

## 8. Conclusion

This paper proposes a three-stage power system restoration methodology considering renewable energy. In each load restoration stage, the goal and tasks

are defined according to power system status. Moreover, a load restoration methodology in each stage is proposed to achieve goal functions. The proposed algorithm can help network operators to establish a load restoration plan and make better decision during the load restoration process.

**Outlook:** In this paper, the maximal load increment in one step does not exceed 5% rated capacity of online generators. However in some cases, this value of maximal load increment is not optimal. In future work, the optimal value of maximal load increment should be determined by considering the load type, network topology, control system of online generators, etc. In each load restoration step, the maximal load increment is also different and can be determined by transient simulation.

## References

- [1] M. M. Adibi and L. H. Fink, Power system restoration planning, *IEEE Trans. Power Syst.* 9 (1) (Feb. 1994) 22–28.
- [2] L. H. Fink, L. Kan-Lee and L. Chen-Ching, From generic restoration actions to specific restoration strategies, *IEEE Trans. Power Syst.* 10 (2) (May. 1995) 745–752.
- [3] M. Adibi, P. Clelland, L. Fink, H. Happ, R. Kafka, J. Raine, D. Scheurer and F. Trefny, Power system restoration—A task force report, *IEEE Trans. Power Syst.* 2 (2) (May. 1987) 271–277.
- [4] M. M. Adibi, J. N. Borkoski and R. J. Kafka, Power system restoration—The second task force report, *IEEE Trans. Power Syst.* 2 (2) (Nov. 1987) 927–933.
- [5] J. J. Ancona, A framework for power system restoration following a major power failure, *IEEE Trans. Power Syst.* 10 (3) (Aug. 1995) 1480–1485.
- [6] E. K. Nielson, M. M. Adibi, O. Barrie, M. E. Cooper, K. W. Heussner, M. E. Robertson, J. L. Scheidt and D. Scheurer, System operations challenges, *IEEE Trans. Power Syst.* 3 (1) (Feb. 1988) 118–126.

- [7] Y. Kojima, S. Warashina, S. Nakamura and K. Matsumoto, Development of a guidance method for power system restoration, *IEEE Trans. Power Syst.* 4 (Aug. 1989) 1219–1227.
- [8] S. A. N. Sarmadi, A. S. Dobakhshari, S. Azizi and A. M. Ranjbar, A sectionalizing method in power system restoration based on WAMS, *IEEE Trans. Smart Grid* 2 (1) (March 2011) 190–197.
- [9] I. Mohanty, J. Kalita, S. Das, A. Pahwa and E. Buehler , Ant algorithms for the optimal restoration of distribution feeders during cold load pickup, in: *Proceedings of the 2003 IEEE Swarm Intelligence Symposium*, 2003.
- [10] V. Kumar, R.K.H.C.I. Gupta and H.O. Gupta , Stepwise restoration of power distribution network under cold load pickup, in: *International Conference on Power Electronics, Drives and Energy Systems*, 2006.
- [11] R. A. Rodriguez J and A. Vargas, Multi-criteria decision considering penalty costs for load restoration in MV networks, in: *IEEE Porto Power Tech Proceedings*, 2001.
- [12] K. Han-Ching Kuo and H. Yuan-Yih, Distribution system load estimation and service restoration using a fuzzy set approach, *IEEE Trans. Power Del.* Vol.8 (Oct. 1993) 1950–1957.
- [13] W. P. Luan, M. R. Irving and J.S. Daniel , Genetic algorithm for supply restoration and optimal load shedding in power system distribution networks, *IEE Proceedings - Generation, Transmission and Distribution* 149 (2) (Mar. 2002) 145–151.
- [14] A. M. El-Zonkoly, Distributed generation approach for single step system restoration during cold load pickup, in: *Transmission and Distribution Conference and Exposition (T&D)*, 2012.
- [15] O. Duque and D. Morinigo, Load restoration in electric distribution networks using a metaheuristic technique, in: *IEEE Mediterranean Electrotechnical Conference*, 2006.



- [16] W. Liu, Z. Lin, F. Wen and G. Ledwich, A wide area monitoring system based load restoration method, *IEEE Trans. Power Syst.* 28 (May. 2013) 2015–2034.
- [17] H. Hijazi and S.Thibaux, Optimal distribution systems reconfiguration for radial and meshed grid, *Electr. Power Energy Syst.* 72 (Nov. 2015) 136–143.
- [18] D. S. Sanches, J. B. A. London, Jr and A. C. B. Delbem, Multi-objective evolutionary algorithm for single and multiple fault service restoration in large-scale distribution systems, *Electr. Power Energy Syst. Res.* 110 (May. 2014) 144–153.
- [19] S. Dimitrijevic and N. Rajakovic, An innovative approach for solving the restration problem in distribuion network, *Electr. Power Syst. Res.* 81 (2011) 1961–1972.
- [20] C. M. Huang, C. T. Hsieh and Y. S. Wang, Evolution of radial basic function neural network for fast restoration of distribution systems with load variations, *Electr. Power Energy Syst.* 33 (2011) 961–968.
- [21] S. P. Singh, G. S. Raju, G. K. Rao and M. Afsari, A heuristic method for feeder reconfiguration and service restoration in distribution networks, *Electr. Power Energy Syst.* 31 (2009) 309–314.
- [22] V. J. Garcia and P. M. Frana, Multiobjective service restoration in electric distribution networks using a local search based heuristic, *Eur. J. Oper. Res.* 189 (2008) 694–705.
- [23] R. Perez-Guerrero, G. T. Heydt, N. J. Jack, B. K. Keel and A. R. Castellano, Jr., Optimal restoration of distribution systems using dynamic programming, *IEEE Trans. Power Del.* 23 (Jul. 2008) 1589–1596.
- [24] P. M. S. Carvalho, L. A. F. M. Ferreira and L. M. F. Barruncho, Optimization appraoch to dynamic restoration of distribution systems, *Electr. Power Energy Syst.* 29 (2007) 222–229.

- [25] J. Machowski, J. W. Bialek and J. R. Bumby, *Power System Dynamics: Stability and Control*, John Wiley, 2008.
- [26] IEEE Recommended Practice for Excitation System Models for Power System Stability Studies.
- [27] B. Ion, *Synchronous generators*, Taylor & Francis Group, LLC, 2006.
- [28] R. Kafka, Review of PJM restoration practices and NERC restoration standards, in: *IEEE Power and Energy Society General Meeting*, 2008.
- [29] C. Shen, P. Kaufmann, and M. Braun, Optimizing the generator start-up sequence after a power system blackout, in: *Proc. IEEE PES General Meeting*, 2014.
- [30] J. Nadira, A. Naida, E. Arslanagic, L. Kurtovic, E. Lagumdzija and N. Novica, Dijkstra's shortest path algorithm serial and parallel execution performance analysis, in: *2012 Proceedings of the 35th International Convention*, 2012.
- [31] L. Yan and G. Xueping, Skeleton-network reconfiguration based on topological characteristics of scale-free networks and discrete particle swarm optimization, *IEEE Trans. Power Syst.* 22 (Aug. 2007) 1267 – 1274.
- [32] C. Wen-Hui, Quantitative decision-making model for distribution system restoration, *IEEE Trans. Power Syst.* 25 (Feb. 2010) 313 – 321.
- [33] W. Chong and V. Vija, *Fuzzy Logic with Engineering Applications*, John Wiley & Sons, 2010.
- [34] Z. Jiangfei, H. TingLei and P. Fei, Genetic algorithm based on greedy strategy in the 0-1 knapsack problem , in: *WGEC '09. 3rd International Conference on Genetic and Evolutionary Computing*, 2009.
- [35] A. Lew and H. Mauch, *Dynamic programming*, Springer, 2007.

- [36] D. E. Goldberg, Genetic algorithms in search, optimization and machine learning, Addison-Wesley, 1989.
- [37] A. M. EI-Zonkoly, Renewable energy sources for complete optimal power system black-start restoration, IET. Gener. Transm.Distrib Vol.9 (2015) 531–539.